

Magnetic properties of diluted magnetic (Gd,Lu)₂O₃

B. Antic, M. Mitric, and D. Rodic

Institute of Nuclear Sciences "Vinca," Laboratory of Solid State Physics, P.O. Box 522, 11001 Belgrade, Yugoslavia

Y. Zhong, Y. Artemov, S. Bogdanovich, and Jonathan R. Friedman*

The City College of New York, Department of Physics, Convent Avenue at 138th Street, New York, New York 10031

(Received 24 November 1997)

The magnetic susceptibility of the diluted magnetic Lu_{2-x}Gd_xO₃ ($x=0.06, 0.10, 0.22, 0.40, 1.00, 1.40, 1.80$) was measured in the temperature range 1.7–295 K. The inverse susceptibility changes slope to a smaller value below 2.2 K for the samples with $x \leq 0.40$. In the cubic Lu_{0.20}Gd_{1.80}O₃ the slope increases below 2.8 K. These changes are attributed to the large difference in susceptibility for two cationic sites at low temperatures and to the crystallographic distribution of Gd³⁺ ions. The monoclinic Lu_{0.20}Gd_{1.80}O₃, which was obtained from the stoichiometrically similar cubic phase at 1620 K, has an antiferromagnetic phase transition at 3.4 K. The magnetic-ion distribution for low-concentration samples ($x=0.06, 0.10$) was studied using an isolated-cluster method in the nearest-neighbor approximation. In these samples a tendency for magnetic-ion cluster formation was found. A random cluster distribution was found to be consistent with the susceptibility data for the sample with $x=0.06$. For the $x=0.10$ sample the susceptibility calculated with a modified cluster distribution gives the best agreement with the experimental results. [S0163-1829(98)00230-6]

I. INTRODUCTION

Solid solutions of the sesquioxides, Lu₂O₃ and Gd₂O₃, have yielded a series of diluted magnets, Lu_{2-x}Gd_xO₃. These solutions are formed from *C*-type cubic structures, where the cations are distributed over two nonequivalent special crystallographic sites: *8b* with local symmetry *C*_{3i} and *24d* with local symmetry *C*₂. O²⁻ ions are in the general *48e* positions.¹ The mixed oxide Lu_{2-x}Gd_xO₃ is expected to be of the same structure type. It is known that the cubic *C*-Gd₂O₃ transforms into a monoclinic *B*-Gd₂O₃ at 1530–1670 K, depending on the heating time.² Lu₂O₃ is usually found in the cubic phase and a transition to a monoclinic phase is possible only at high pressures and temperatures.³

The Lu³⁺ ion has a ground state ⁸S₀ so that Lu₂O₃ is a diamagnetic. The Gd³⁺ ion has a ⁸S_{7/2} ground state. Hence, Gd³⁺ is an isotropic ion ($L=0$) and its magnetic properties originate from the spin only. Cubic Gd₂O₃ has a complex antiferromagnetic structure below 1.6 K,⁴ while monoclinic Gd₂O₃ has an antiferromagnetic transition at 3.4 K.⁵ For *S*-state ions the influence of the crystal field is predicted by group theory.⁶ Van Vleck and Penny have suggested that the splitting of a "spin-only" ion is caused by a second-order interaction between the crystal field and the spin-orbit coupling vector.⁶ Theoretical calculation and experiments show a small crystal-field splitting of ⁸S_{7/2} ground state in the Gd³⁺ compound.⁴ Thus, the Lu_{2-x}Gd_xO₃ system is ideal for the study of the influence of crystal structure on magnetic properties. Also, through the synthesis of mixed oxides in a wide concentration range, it is possible to study these systems in both high and low concentration regions. In this paper we present a study of the magnetic susceptibility of several samples of Lu_{2-x}Gd_xO₃ with $0.06 \leq x \leq 1.80$.

II. EXPERIMENT

A. Sample preparation and x-ray characterization

The Lu_{2-x}Gd_xO₃ samples ($x=0.02, 0.06, 0.10, 0.22, 0.40, 1.00, 1.40, 1.80$) were obtained starting from Lu₂O₃ (99.99%) and Gd₂O₃ (99.9%). Mixtures of these oxides were dissolved in HNO₃. Precipitation of the appropriate hydroxides was achieved by the addition of NH₄OH. The precipitates were washed in distilled water, dried and milled. The powders were pressed under 0.2 GPa and fired at 1370 K for 24 h. The samples were sintered at 1470 K for 24 h. The sintering process was monitored by x-ray diffraction. The samples obtained were single (cubic) phase with the same structure as the starting oxides.

To obtain monoclinic Lu_{2-x}Gd_xO₃, samples in the cubic phase were fired at 1620 K for 10 h. This method produced a sample of Lu_{0.20}Gd_{1.80}O₃ that was fully transformed into the *B* phase. However, all other compositions remained in the cubic phase without any admixture of monoclinic phase.

X-ray diffraction was performed using a Phillips diffractometer with Cu *K*α radiation. In order to use x-ray data for crystal structure refinement three samples (*C*-Lu_{0.20}Gd_{1.80}O₃, *B*-Lu_{0.20}Gd_{1.80}O₃, and *C*-Lu_{1.80}Gd_{0.20}O₃) were recorded from 10.00 to 110.00° in 2θ, with a step spacing of 0.02° and exposure of 10 s/step. The other samples were recorded in the range 10.00–80.00°, with a step spacing of 0.02° in 2θ and exposure of 5 s/step.

B. Magnetic-susceptibility measurements

The magnetic susceptibility of Lu_{2-x}Gd_xO₃ samples was measured in the temperature range 1.7–295 K using a Quantum Design MPMS-5 superconducting quantum interference device magnetometer. In Gd₂O₃ at 4.3 K, where short-range magnetic order was found, the susceptibility was independent of magnetic field up to 18 kOe, while at 1.8 K the

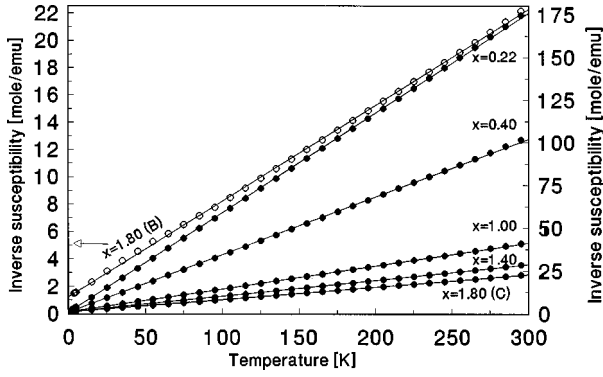


FIG. 1. Inverse molar magnetic susceptibility versus temperature for cubic $\text{Lu}_{2-x}\text{Gd}_x\text{O}_3$ ($x \geq 0.22$) and for monoclinic $\text{Lu}_{0.20}\text{Gd}_{1.80}\text{O}_3$ samples. Symbols are experimental data and lines are fits to the Curie-Weiss law.

susceptibility at 18 kOe was slightly smaller than at 6 and 12 kOe.⁴ Thus the susceptibility of the diluted magnetic $\text{Lu}_{2-x}\text{Gd}_x\text{O}_3$ was expected to be independent of magnetic field and we have measured it in only one magnetic field of 1 T. The paramagnetic susceptibility was obtained by subtracting the diamagnetic contribution from the experimental data. The diamagnetic contribution was calculated using ionic diamagnetic values, -20×10^{-6} , -17×10^{-6} , and -12×10^{-6} emu/mol for Gd^{3+} , Lu^{3+} , O^{2-} ,⁷ respectively. The temperature dependence of the inverse paramagnetic susceptibility of $\text{Lu}_{2-x}\text{Gd}_x\text{O}_3$ is shown in Figs. 1, 2, 4, and 5.

III. RESULTS AND DISCUSSION

A. Crystal structure parameters of $(\text{Lu,Gd})_2\text{O}_3$ samples

The x-ray-diffraction data show that the cubic $\text{Lu}_{2-x}\text{Gd}_x\text{O}_3$ samples crystallize in the space group $Ia\bar{3}$ and bixbyite structure type (C -type). The diffraction data for sample $B\text{-Lu}_{0.20}\text{Gd}_{1.80}\text{O}_3$ correspond to $B\text{-Gd}_2\text{O}_3$,⁸ which crystallizes in the space group $C2/m$. According to the data from Ref. 9, in the B phase the cations occupy three kinds of $4i$ positions, the oxygen ions are in four different $4i$ positions and one oxygen ion is in $2a$ position. We tried to refine the crystal structures of $\text{Lu}_{2-x}\text{Gd}_x\text{O}_3$, but large standard deviations in atomic parameters were obtained because of the similarity of the scattering factors of the two cations: The scattering factors are proportional to the square of the atomic numbers Z ($Z=64$ and $Z=71$ for Gd and Lu, respectively). Gd is a good neutron absorber and, consequently, neutron diffraction is also an unsuitable probe of the detailed crystal structure of $\text{Lu}_{2-x}\text{Gd}_x\text{O}_3$ samples. The lattice parameters for $C\text{-Lu}_{2-x}\text{Gd}_x\text{O}_3$ and $B\text{-Lu}_{0.20}\text{Gd}_{1.80}\text{O}_3$ were determined from x-ray data and are listed in Table I. The lattice constants for the cubic-phase samples follow the Vegard's rule:

$a(x) = a_0 + bx = 10.383(1) + 0.210(2)x$, where the coefficient b reflects the difference in cationic radii [$\delta r = r(\text{Gd}^{3+}) - r(\text{Lu}^{3+}) = 2b/4 = 2 \cdot 0.210/4 = 0.105 \text{ \AA}$ (Ref. 10)]. The monoclinic B phase, $x=1.80$ sample has a density of 8.59 g/cm^3 , as compared to 7.79 g/cm^3 for the corresponding C phase. The change of density as well as the abrupt change of symmetry show that the phase transition is of the first order: the $C \rightarrow B$ transition in $\text{Lu}_{0.20}\text{Gd}_{1.80}\text{O}_3$ is irreversible.

B. Magnetic susceptibility of $(\text{Lu,Gd})_2\text{O}_3$ samples

The low-temperature magnetic susceptibility data of $\text{Lu}_{2-x}\text{Gd}_x\text{O}_3$ are shown in Figs. 2(a)–2(c). For samples with $x \leq 0.40$ the slope of $\chi^{-1}(T)$ decreases abruptly when the temperature falls below 2.2 K. In the samples with $x=1.00$ and $x=1.40$ no change of slope was found in the measured range of temperature. In the cubic sample with $x=1.80$, there is a sudden increase in the slope of $\chi^{-1}(T)$ below 2.8 K.

Data for the magnetic susceptibility of $\text{Lu}_{2-x}\text{Gd}_x\text{O}_3$ were fitted to a Curie-Weiss law, $\chi(T) = C_M(x)/[T - \theta(x)]$, where the fitting parameters C_M and θ are the Curie molar constant and Curie-Weiss temperature, respectively. The data for samples $x=1.80(C)$ and $x \leq 0.40$ were analyzed in two parts, for temperatures above and below the change in slope of $\chi^{-1}(T)$ shown in Fig. 2.

The values of $C_M(x)$ obtained from the high-temperature data are given in Table II. The dependence of C_M on x is linear, $C_M(x) = C_{M0}x = 7.70(8)x$. The calculated effective magnetic moments, $\mu_{1\text{eff}}^2 = 8C_M(x)/x(\mu_B)$, also listed in Table II, are close to the value for the free ion ($7.94\mu_B$). The spin values (S) listed in Table II are close to the value for Gd^{3+} ($4f^7$ configuration). The effective magnetic moments $\mu_{2\text{eff}}$ calculated from the low-temperature susceptibility data differ from $\mu_{1\text{eff}}$ values. This difference will be discussed below.

The Curie-Weiss temperatures for all samples were found to be negative, indicating a predominance of antiferromagnetic interaction between Gd^{3+} ions. From high-temperature susceptibility data a linear dependence of $\theta(x)$ was obtained, $\theta(x) = \theta_0 x + \text{const}$, with $\theta_0 = (8.8 \pm 0.4) \text{ K}$ and $\text{const} = 0$ (within experimental error). A plot of $\theta(x)$ versus x is shown in Fig. 3. Extrapolation to $x=2.00$, gives $\theta(\text{Gd}_2\text{O}_3) = -17.6 \text{ K}$, which compares well with earlier experimental values of -18.7 K (Ref. 11) and -17 K .¹² The data in Fig. 3 show that the B and C phases for $\text{Lu}_{0.20}\text{Gd}_{1.80}\text{O}_3$ have different values of θ , which can be explained in terms of the coordination of magnetic ions in cubic and monoclinic samples. The cations in the C phase have six oxygen ions in the first and 12 cations in the second coordination sphere, respectively. Three cations in B phase have seven oxygen

TABLE I. Unit-cell parameters of $\text{Lu}_{2-x}\text{Gd}_x\text{O}_3$.

Cubic $\text{Lu}_{2-x}\text{Gd}_x\text{O}_3$								
x	0.02	0.06	0.10	0.22	0.40	1.00	1.40	1.80
a (Å)	10.3874(4)	10.3944(3)	10.4037(3)	10.4280(1)	10.4648(2)	10.5916(4)	10.6731(3)	10.7648(2)
Monoclinic $\text{Lu}_{0.20}\text{Gd}_{1.80}\text{O}_3$								
$a = 14.016(9) \text{ \AA}$, $b = 3.54(2) \text{ \AA}$, $c = 8.70(6) \text{ \AA}$, $\beta = 100.26(2)^\circ$, $V = 424.4 \text{ \AA}^3$								

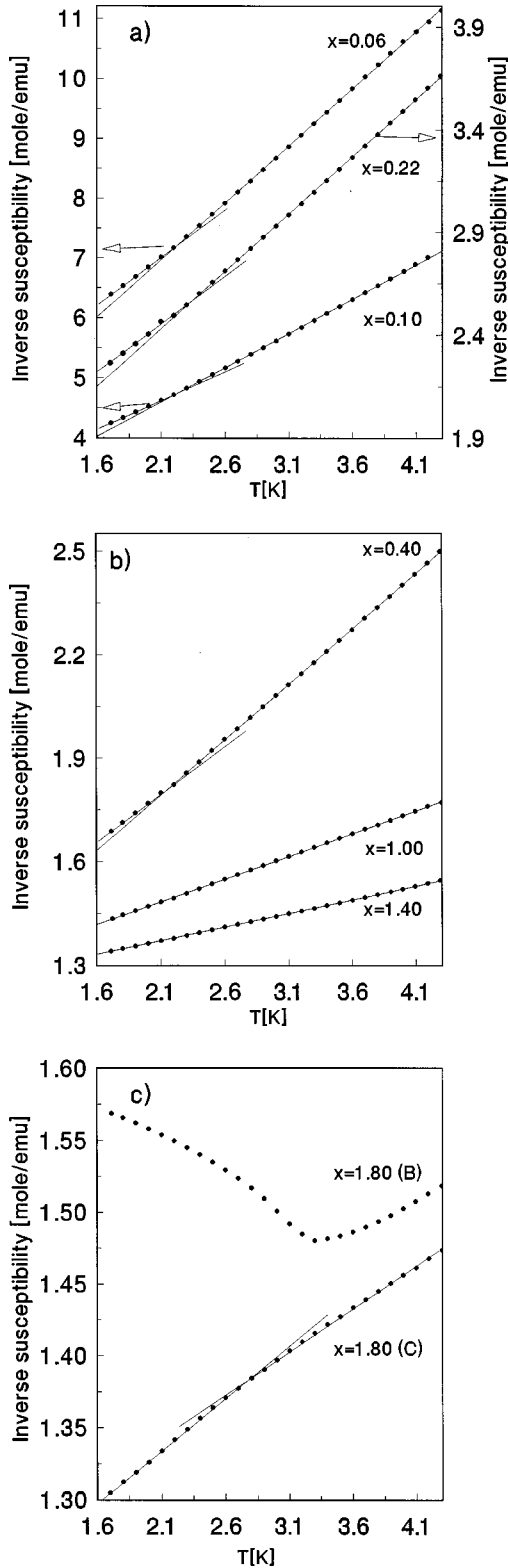


FIG. 2. Low-temperature susceptibility for cubic $\text{Lu}_{2-x}\text{Gd}_x\text{O}_3$ ($0.02 \leq x \leq 1.80$) samples and for monoclinic $\text{Lu}_{0.20}\text{Gd}_{1.80}\text{O}_3$ samples. Note the different ordinates for different samples. In (c) *B* denotes the monoclinic phase and *C* denotes the cubic phase.

ions in the first coordination spheres. Each cation has 12 cationic neighbors in the second coordination sphere.¹⁰ The number of superexchange paths (cation-anion-cation) as well as their geometry (bond lengths and angles) differ in two phases. Assuming that superexchange is the dominant inter-

action mechanism, the difference in θ values for the *C*- and *B*- $\text{Lu}_{0.20}\text{Gd}_{1.80}\text{O}_3$ reflects a stronger interaction among magnetic ions in the monoclinic sample caused by the difference in number of paths, angles, and bonds.

The mean exchange integral for cubic $\text{Lu}_{2-x}\text{Gd}_x\text{O}_3$ can be calculated from the θ values using the relation

$$\frac{J_{\text{eff}}}{k_B} = \frac{3\theta(x)}{z_x S(S+1)}, \quad (1)$$

where z denotes the number of cationic neighbors ($z=12$). J_{eff}/k_B was calculated to be 0.140 K in good agreement with results obtained by Moon and Koehler in Gd_2O_3 :⁴ $J_{8b-24d}/k_B=0.1328$ K and $J_{24d-24d}/k_B=0.1414$ K.

The observed change in slope of χ^{-1} vs T can be caused by two effects: (a) the crystal-field influence on Gd^{3+} ions and (b) mutual influence of the difference in the temperature dependence of the susceptibility for each cationic site at low temperatures and type of crystallographic distribution. In Gd^{3+} compounds the crystal-field effect is of second order and acts on magnetic properties at the low temperatures. The crystal field of the C_2 and C_{3i} symmetry in *C*- Gd_2O_3 splits the ground term $^8S_{7/2}$ of Gd^{3+} ions into four doublets.¹³ Starting from the assumption that the changes in slope observed in Fig. 2 are caused by the population of the highest levels in Gd^{3+} ions, it can be shown that the slope of the calculated inverse susceptibility only increases as the temperature is decreased. This calculation was done taking into account the states of Gd^{3+} ions given in Ref. 13. Hence, the observed decrease in slope found at low temperatures for samples $x \leq 0.40$ cannot be due to the crystal-field effect. In addition, the local-site symmetry is the same for all samples and thus the same temperature dependence for $\chi^{-1}(T)$ is expected. Finally, earlier work indicates that the crystal-field splitting of the $^8S_{7/2}$ ground term of Gd^{3+} ions in Gd_2O_3 is smaller than the lowest measured temperature (1.7 K).^{4,13} For all of these reasons we can exclude the crystal-field as a cause for the change of slope in the temperature dependence of $\chi^{-1}(T)$ in $\text{Lu}_{2-x}\text{Gd}_x\text{O}_3$.

A study of cubic Gd_2O_3 by polarized and unpolarized neutrons showed a complex magnetic behavior in the paramagnetic phase.⁴ Diffuse scattering of unpolarized neutrons at 4.3 K revealed the existence of the short-range magnetic order, or nonzero correlations of spins on different sites. It was found that only first-neighbor and second-neighbor correlations are different from zero.⁴ Also, a difference in the susceptibility of Gd^{3+} ions at the *8b* and *24d* sites, found below 10 K, increases with decreasing temperature.⁴ An approximate theory for susceptibility based on spin correlations, predicts a temperature dependence of the inverse susceptibility for *8b* and *24d* sites in Gd_2O_3 , which is similar to the one for *C*- $\text{Lu}_{0.20}\text{Gd}_{1.80}\text{O}_3$, shown in Fig. 4. The $\chi^{-1}(T)$ dependence (Fig. 4) for both cationic sites was explained in Ref. 4, where it was supposed that there is a strong tendency of ions to form antiferromagnetic clusters in *24d* sites, reducing the susceptibility of these ions. At the same time, antiferromagnetic interactions between *8b*-*24d* ions decrease and, as a consequence, susceptibility of *8b* ions increases. We consider difference in susceptibility of the Gd^{3+}

TABLE II. Molar Curie's constants, spins, and effective magnetic moments of Gd^{3+} ions in $Lu_{2-x}Gd_xO_3$.

x	0.06	0.10	0.22	0.40	1.00	1.40	1.80(C)	1.80(B)	2.00[**]
C_M (emu K/mole)	0.45	0.767	1.65	2.97	7.46	10.87	13.89	14.29	
$\mu_{1\text{ eff}} (\mu_B)$	7.75	7.83	7.75	7.70	7.73	7.88	7.86	7.97	7.85
$\mu_{2\text{ eff}} (\mu_B)$	9.16	9.13	9.11	8.45			7.80		6.08
S_{exp}	3.42	3.44	3.48	3.41	3.41	3.49	3.48	3.54	

ion at the $8b$ and $24d$ sites together with cation distribution as a possible mechanism responsible for the change of slope in $\chi^{-1}(T)$ of $Lu_{2-x}Gd_xO_3$.

As noted above, the temperature dependence of χ^{-1} for $C-Lu_{0.20}Gd_{1.80}O_3$ has a change in slope at 2.8 K (Fig. 2). Similar behavior was obtained for both stoichiometric and substoichiometric $C-Gd_2O_3$ at 2.8 K.⁵ The magnetic susceptibility for each site in $C-Lu_{0.20}Gd_{1.80}O_3$ was calculated using an approximate theory proposed for Gd_2O_3 .⁴ The calculation predicts a linear susceptibility: $\chi_{8b,24d}^{(Lu_{0.20}Gd_{1.80}O_3)}(T) = 0.9\chi_{8b,24d}^{(Gd_2O_3)}(T)$, reflecting the fact that 10% of Gd^{3+} ions have been replaced by Lu^{3+} . This theory is valid only above $T \approx 3$ K.⁴ Around 3 K and below, experimental values of the susceptibility of Gd_2O_3 (Ref. 4) were used to obtain the temperature dependence of the susceptibility for both sites in $C-Lu_{0.20}Gd_{1.80}O_3$, $\chi_{8b}(T)$ and $\chi_{24d}(T)$. Experimental low-temperature susceptibility data for $C-Lu_{0.20}Gd_{1.80}O_3$ were fit to $\chi(T) = w_1\chi_{8b}(T) + w_2\chi_{24d}(T)$. Satisfactory agreement was obtained for $w_1 = 0.27$ and $w_2 = 0.73$, as shown in Fig. 4 (values are given for a half mole). This fit confirms the existence of spin correlations between Gd sites and indicates a random crystallographic cationic distribution in $C-Lu_{0.20}Gd_{1.80}O_3$. For ideally random system, the coefficients w_1 and w_2 should be 0.25 and 0.75, respectively, because ratio of crystallographic sites is 1:3. For samples with $x < 1.80$ the dependence $\chi_{8b}^{-1}(T)$ and $\chi_{24d}^{-1}(T)$ are unknown and we cannot treat the situation quantitatively. Samples with $x = 1.00$ and 1.40 show simple paramagnetic behavior down to 1.7 K [see Fig. 2(b)]. Both spin correlations and cationic distribution results in behavior be-

low 2–3 K. For smaller x (larger dilutions) in the $Lu_{2-x}Gd_xO_3$ samples, isolated clusters of magnetic ions are formed, as discussed below. In these isolated clusters similar magnetic behavior can be expected.

At temperatures below the change in slope of $\chi^{-1}(T)$ (or at the lowest temperature), the inverse susceptibility of $Lu_{2-x}Gd_xO_3$ decreases linearly with temperature (Fig. 2). If Gd^{3+} ions occupy only one site exclusively then a deviation from linearity would be expected. Thus, the observed linearity of $\chi^{-1}(T)$ indicates replacement of Lu^{3+} ions by Gd^{3+} in both cationic sites.

The aforementioned difference between magnetic moments $\mu_{1\text{ eff}}$ and $\mu_{2\text{ eff}}$ (Table II) is related to the fact that $\chi^{-1}(T)$ differs for two cationic sites. In both $C-Lu_{0.20}Gd_{1.80}O_3$ and Gd_2O_3 ,⁵ the effective magnetic moments satisfy $\mu_{1\text{ eff}} > \mu_{2\text{ eff}}$. This is a consequence of the difference in the temperature dependence of $\chi_{8b}^{-1}(T)$ and $\chi_{24d}^{-1}(T)$ below the bend in $\chi^{-1}(T)$ (Fig. 2). The opposite case ($\mu_{1\text{ eff}} < \mu_{2\text{ eff}}$) is found in mixed samples with $x \leq 0.40$. We suggest this might be caused by a preferential crystallographic distribution of the cations.

The B -phase sample with $x = 1.80$ exhibits a minimum in $\chi^{-1}(T)$ at 3.4 K, indicating a paramagnetic \rightarrow antiferromagnetic phase transition. In Ref. 5 the same type of transition was found both for stoichiometric (at 3.9 K) and substoichiometric (at 3.4 K) monoclinic gadolinium oxides. The cubic gadolinium oxide has antiferromagnetic structure below 1.6 K.⁴ A paramagnetic \rightarrow antiferromagnetic phase transition may exist below 1.6 K for the cubic sample with $x = 1.80$. This result shows stronger magnetic interactions in

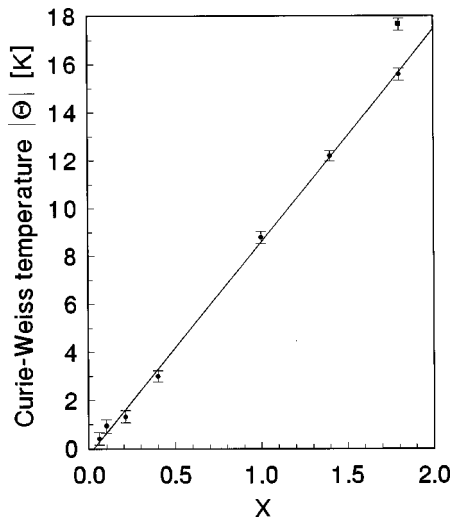


FIG. 3. Curie-Weiss temperature versus magnetic ion concentration: (●) for $C-Lu_{2-x}Gd_xO_3$ and (■) for $B-Lu_{0.20}Gd_{1.80}O_3$.

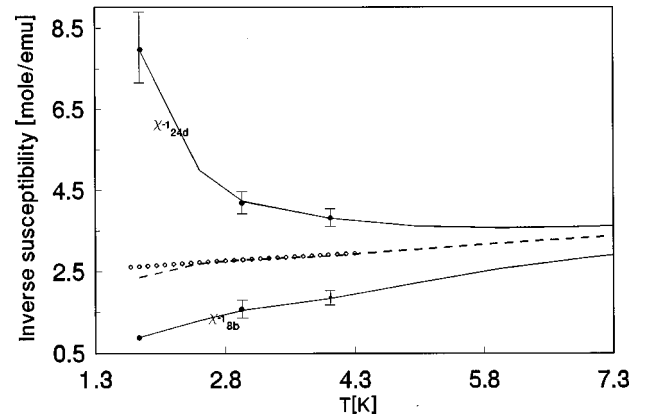


FIG. 4. Comparison of calculated susceptibility (dashed line) versus experimental data (open circle) for $C-Lu_{0.20}Gd_{1.80}O_3$. Inverse susceptibilities for $8b$ and $24d$ sites (solid lines) of $C-Lu_{0.20}Gd_{1.80}O_3$ as a function of temperature were found by using theoretical and experimental results for Gd_2O_3 from Ref. 4.

the B phase than the C phase, also indicated by Curie-Weiss temperatures, $\theta(B\text{-Lu}_{0.20}\text{Gd}_{1.80}\text{O}_3) > \theta(C\text{-Lu}_{0.20}\text{Gd}_{1.80}\text{O}_3)$ shown in Fig. 3.

C. Cluster formation of Gd^{3+} ions in low-concentrated $(\text{Lu}, \text{Gd})_2\text{O}_3$ samples

Results for low-concentration samples were analyzed using the isolated-cluster model in the nearest-neighbor approximation. We shall give here only a brief summary of the model. The model supposes that magnetic Gd^{3+} ions form small clusters that consist of one, two, three, or more magnetic ions. The exchange interaction between ions within each cluster is of the Heisenberg type and interaction between clusters are negligible.¹⁴ The total magnetic susceptibility of the crystal is given as the sum of contributions from different “finite-size” clusters:

$$\chi(T) = \sum_i w_i \chi_i(T), \quad (2)$$

where w_i is the probability of finding a Gd^{3+} ion in a cluster and the susceptibility of the type i cluster is given by^{14,15}

$$\chi_i(T) = \frac{(g\mu_B)^2}{k_B T} \left(\frac{\sum_{\{q\}} \sum_m m^2 \exp(-E_{i\{q\}}/k_B T)}{\sum_{\{q\}} \sum_m \exp(-E_{i\{q\}}/k_B T)} - \left[\frac{\sum_{\{q\}} \sum_m m \exp(-E_{i\{q\}}/k_B T)}{\sum_{\{q\}} \sum_m \exp(-E_{i\{q\}}/k_B T)} \right]^2 \right). \quad (3)$$

In this expression m denotes the magnetic quantum number and the $E_{i\{q\}}$ are the energy eigenvalues of the Hamiltonian for type- i clusters. The Hamiltonian and corresponding eigenvalues for different cluster types are given by Okada.¹⁶

Superexchange is the dominant interaction mechanism in these samples.⁴ The strongest interactions are cation ($24d$)-anion-cation ($24d$) and cation ($8b$)-anion-cation ($24d$). The other cation-cation bonds are formed via two or more oxygen ions and are therefore less important.¹⁷ Thus, in the calculation of the susceptibility we will consider only the nearest-neighbor interactions between Gd^{3+} ions, neglecting the weak next-nearest-neighbor interactions.

The susceptibility of low-concentration samples, $x=0.06$ and $x=0.10$, was calculated using the isolated-cluster method and the results are compared with experimental data in Fig. 5. The Gd^{3+} ions in $8b$ and $24d$ positions have 12 cationic neighbors (next-nearest neighbors). If one takes the free-cationic coordinate for the $24d$ position [$z = -0.0320$ (Ref. 17)] to be zero then the lattice reverts to a face-centered-cubic (fcc) type. The susceptibility was calculated using Eqs. (2) and (3). Experimentally, the most frequently obtained Lande g factor for Gd^{3+} ion is 1.99. This value and the value of $J_{\text{eff}}/k_B = 0.140$ K for exchange integral were used in Eq. (3). The probability that a magnetic ion is in a type- i cluster in an fcc lattice for random cluster distribution is given by¹⁸ $(1-y)^{12}$ for singles (S), $12y(1-y)^{18}$ for pairs (P), $18y^2(1-y)^{23}[5(1-y)+2]$ for open triplet (T_o), and $24y^2(1-y)^{22}$ for close triplet (T_c), where $y=x/2$ for our samples.

Calculated susceptibilities for the predicted random distribution of Gd^{3+} ions are shown for both samples in Fig. 5 (short dash line) and compared with experimental values.

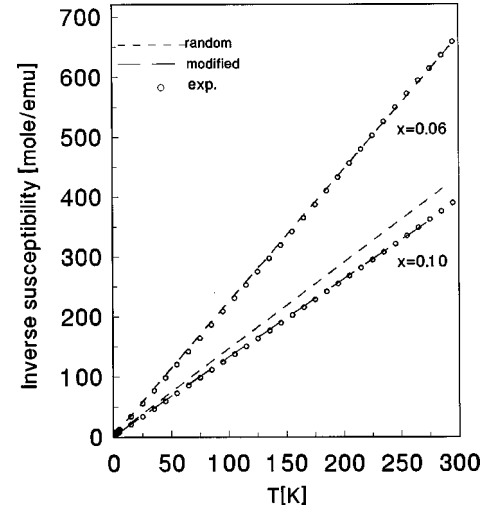


FIG. 5. Inverse magnetic susceptibility vs temperature of $\text{Lu}_{2-x}\text{Gd}_x\text{O}_3$ ($x=0.06$, $x=0.10$). The symbols represent experimental values and the lines are calculated for different types of cluster distribution.

Satisfactory agreement between experimental and calculated values is found for the sample $x=0.06$ but not for the sample $x=0.10$. The probabilities of finding a type- i cluster given a random distribution are presented in Table III for the two measured samples. In the modified distribution, the probabilities for clusters formation are adjustable parameters. The modified distribution yields good agreement with experiment values for the sample $x=0.10$, as shown by the long-dashed line in Fig. 5. For this sample our results indicate a higher propensity for pair formation.

At low temperatures the magnetic behavior of ions in $8b$ and $24d$ sites becomes different and complex. The applied theoretical model, introduced for magnetic systems with one cationic site, does not take into account the difference in the crystallographic positions of ions that form the clusters. For that reason our calculations were carried out above 3 K where the difference in site susceptibilities is negligible.

IV. CONCLUSION

The diluted magnetic $\text{Lu}_{2-x}\text{Gd}_x\text{O}_3$ (cubic phase) was obtained with a wide range of Gd concentration. At a temperature of 1620 K and under pressure of 0.2 GPa only the sample with the highest Gd^{3+} ion concentration ($x=1.80$) was transformed into a monoclinic phase. The C and B phases of $\text{Lu}_{0.20}\text{Gd}_{1.80}\text{O}_3$ show magnetic behavior similar to the corresponding phases of Gd_2O_3 : the monoclinic (B)

TABLE III. Probability values for different cluster types, assuming different types of magnetic-ion distribution.

$x=0.06$				
Cluster type	S	P	T_o	T_c
Random	0.69	0.21	0.057	0.011
$x=0.10$				
Random	0.54	0.24	0.10	0.02
Modified	0.51	0.38	0.10	0

sample undergo a paramagnetic→antiferromagnetic phase transition, and in the cubic (*C*-phase) samples, $\chi^{-1}(T)$ exhibits a change of slope as a function of temperature.

Crystal-field effects on the Gd^{3+} ions in $\text{Lu}_{2-x}\text{Gd}_x\text{O}_3$ are excluded as possible mechanism for the change in slope in the measured range of temperature. The change in slope in *C*- Gd_2O_3 (Ref. 5) (similar to that in *C*- $\text{Lu}_{0.20}\text{Gd}_{1.80}\text{O}_3$) was previously attributed to a Schottky anomaly.⁵ We have argued that the bend in $\chi^{-1}(T)$ is produced by a different mechanism, namely, combination of the large difference in susceptibility of two cationic sites at low temperatures and crystallographic distribution of Gd^{3+} ions.

The distribution of magnetic Gd^{3+} ions in *C*- $\text{Lu}_{2-x}\text{Gd}_x\text{O}_3$ can be described in terms of: (a) crystallographic distribution of Gd^{3+} ions over *8b* and *24d* cationic sites and (b) cluster formation. The x-ray-diffraction data could not yield the crystallographic distribution because of the similar scattering

factors of Gd^{3+} and Lu^{3+} ions. Magnetic data showed that Gd^{3+} ions replace Lu^{3+} ions in both cationic sites. A random crystallographic distribution was found in the sample with $x=1.80$ (cubic). We assume that in $x\leq 0.40$ samples Gd^{3+} ions are preferentially located on one crystallographic site. The effect of cluster formation in low-concentration samples was explored through a calculation of the magnetic susceptibility using the isolated-cluster method. The results indicate that the sample with $x=0.06$ is consistent with a random cluster distribution of Gd^{3+} ions, while for the sample with $x=0.10$ the probability for singles is smaller and the probability for pairs larger.

ACKNOWLEDGMENT

The authors thank Professor M. P. Sarachik for allowing us to use laboratory equipment.

*Present address: Department of Physics and Astronomy, SUNY-Stony Brook, Stony Brook, NY 11794-3800.

¹M. Marezio, *Acta Crystallogr.* **20**, 723 (1966).

²G. Brauer, in *Progress in the Science and Technology of the Rare Earths*, edited by L. Eyring (Pergamon, Oxford, 1968), Vol. 3, p. 434.

³R. H. Hoekstra, *Inorg. Chem.* **5**, 754 (1965).

⁴M. R. Moon and C. W. Koehler, *Phys. Rev. B* **11**, 1609 (1975), and references therein.

⁵E. A. Miller, J. F. Jelinek, A. K. Gschneidner, and C. B. Gerstein, Jr., *J. Chem. Phys.* **55**, 2647 (1971).

⁶H. Hacker, S. M. Lin, Jr., and F. E. Westrum, Jr., in *Rare Earth Research-III*, edited by L. Eyring (Gordon & Breach, New York, 1965), p. 93, and references therein.

⁷C. P. Selwood, *Magnetochemistry* (Interscience, New York, 1956), p. 78.

⁸J. O. Guentert and L. R. Mozzi, *Acta Crystallogr.* **11**, 746 (1958).

⁹L. H. Yakel, *Acta Crystallogr., Sect. B: Struct. Crystallogr. Cryst. Chem.* **35**, 564 (1979).

¹⁰B. Antic, M. Mitric, and D. Rodic, *J. Phys.: Condens. Matter* **9(2)**, 365 (1997).

¹¹A. N. Smol'kov and V. N. Dobrovol'skaya, *Neorg. Mater.* **1**, 1564 (1965).

¹²S. Arajis and V. R. Colvin, *J. Appl. Phys.* **33**, 2517 (1962).

¹³E. Antic-Fidancev, M. Lemaitre-Blaise, and P. Caro, *J. Chem. Phys.* **15**, 2906 (1982).

¹⁴S. J. Smart, in *Magnetism*, edited by G. T. Rado and H. Suhl (Academic, New York, 1963), Vol. 3, p. 69.

¹⁵V. Kusigerski, M. Mitric, V. Spasojevic, D. Rodic, and A. Bajorek, *J. Magn. Magn. Mater.* **128**, 369 (1993).

¹⁶O. Okada, *J. Phys. Soc. Jpn.* **48**, 391 (1980).

¹⁷B. Antic, M. Mitric, and D. Rodic, *J. Magn. Magn. Mater.* **145**, 349 (1994).

¹⁸E. R. Behringer, *J. Chem. Phys.* **29**, 537 (1958).